Solid Earth Discuss., 3, C340–C348, 2011
www.solid-earth-discuss.net/3/C340/2011/

Solid Earth Discussions

Interactive comment on "Metamorphic history and geodynamic significance of the Early Cretaceous Sabzevar granulites (Sabzevar structural zone, NE Iran)" *by* M. Nasrabady et al.

M. Nasrabady et al.

rossetti@uniroma3.it

Received and published: 8 September 2011

Both reviewers provided constructive comments that will help to improve the original ms. In the following, we will provide a detailed response to the Reviewers's comments together with a list of the changes that we will consider in the revised typescript.

Referee #1, Prof. M. Bröcker -Points 1-2. The reviewer finds that our manuscript lacks of (i) a detailed petrographical description of the samples used for geochemistry and (ii) synthetic illustration of the thermobarometric results. Following the rev. advice, we have prepared three tables, where we have provided this information (see attached Tables).

-Point 3. The mentioned K-Ar and Rb-Sr ages pertain to the ophiolitic sequences of the Sabzevar structural zone hosting the granulite complex as a tectonic slice. The hosting ophiolitic sequence has a Late Cretaceous formation (Shojaat et al., 2003) and Tertiary deformation ages (Barotz et al., 1978) The granulites bodies that are the object of this study are thus an exotic fragment(s) within the Tertiary Sabzevar structural zone. We agree with the arguments stated by the Referee, and we will modify the text in order to better clarify these points . The Late Cretaceous formation age for the Sabzevar ophiolitic domain was already introduced on line 20 at pg. 3 along with the relevant references.

-Point 4. We will consider the MORB affinity in the discussion section.

-Point 5. We thank Prof. Bröcker for the new information and age data on the Sistan metamorphism. These new Rb-Sr Late Cretaceous ages for the metamorphic peak in the Sistan suture rule out any possible connection with the proto-Sabzevar subduction. Nevertheless, we would emphasise here that connection with the Sistan subduction was only tentative and based on the early available geochronological data set. In the revised version, we will carefully reconsider the proposed regional scenario in the light of the new Rb-Sr data set provided by Prof. Brocker.

-Point 6. Ellipses refer to THERMOCALC outputs as obtained from different samples. We will specify this information in the revised version of Figure 10. For what concerns Figure 12, we agree that some confusion can arise from this representation. Our aim was to indicate the relevant P-T fields for the prograde M2 evolution by using representative thermobarometric results. We will correct this representation, just depicting the corresponding P-T fields as deduced from Figure 10.

-Point 7. We have performed, as specified in the submitted typescript, geochemical analyses at Acivation laboratories in Canada. We will specify analytical details in the revised version.

-Point 8-9 and following comments. We have checked the technical and typo errors,

including the reference format. We agree with all the detailed suggestions and advice from the reviewer for what concerns figures and tables and we will change the manuscript accordingly.

Anonymous Referee #2 Major points of criticism from Referee #2 concern (i) the petrographical description (particularly for what concerns the garnet inclusion assemblages and garnet chemistry) and (ii) the quality of the forward modelling (pseudosection approach for what pertains the “effective reactive bulk composition”). Both points may hamper the correct reconstruction of the P-T path followed by a metamorphic unit (anticlockwise in this study) if not carefully taken into account.

(i)) We agree with the Rev. that caution should be considered when evaluating the inclusion assemblage in high-grade terrains. Nevertheless, our detailed investigations carried out on several thin sections of different samples systematically reveal consistent inclusion assemblages in prograde garnet, being amphibole-titanite/ilmenite-plagioclase-quartz $\pm$ epidote the inclusion assemblage at garnet core and rutile instead of titanite and cpx instead of amphibole present at the garnet rim. This textural evidence is clearly illustrated in Figure 4, where the overgrowth of rutile onto former titanite/ilmenite aggregates are documented. This strongly supports the prograde evolution proposed in the submitted typescript, being compatible with continuous garnet growth along an prograde P-T gradient from amphibolite to granulite facies. A support to this interpretation is given by the thermobaric calculations obtained from the inclusion assemblage found at the garnet cores that systematically provided lower P-T estimates than those obtained from the garnet rim inclusion assemblages and compatible with the scenario depicted above (cfr. Fig. 10 of the submitted typescript). For what concerns the garnet chemistry, we agree with the referee that a more accurate description of the garnet zoning have to be taken into account in the revised typescript. Nevertheless, we would emphasise here that in the submitted text (cfr. pg 8, lines 3-24), we have stated that different zonation patterns are present and that various degrees of diffusion/resorption portion may have influenced the garnet zoning. Since

we were interested in constraining the prograde and peak conditions, for thermobarometric estimates and pseudosection calculations we have thus selected those grains (and hence samples) that did not provide evidence for significant retrograde resorption. What is important to emphasise here, in agreement with the referee interpretation, it is the fact that the garnet composition and zoning pattern reflect different (individual) stages of growth during the general P-T evolution and only grains such as EG354_Gt4 reflects the entire evolution. We will take into consideration this topic in the revised version, better delineating the different types of garnet zonation and the growth types.

(ii) The paragenesis gt+cpx+fsp+qz quoted by Referee#2 actually does not occur at 500°C and 3 kbar. Ubiquitary is in fact presence of amphibole, whereas the coexisting Ti-phase, ilmenite or rutile is indicative for low and high-pressure conditions, respectively. Preservation of Cpx at low pressure/low temperature is just a consequence of water-deficient conditions resulting from the considered water content of the bulk rock composition. This concern is specified in the submitted typescript (cfr. lines 19-25 in pg 15). We agree with the reviewer that the issue of the garnet composition and the “real bulk reactive composition” introduce uncertainty on the derived P-T data. However, there are further and more important aspects to be discussed such as the unknown amount of melt extracted, incomplete equilibrium (involving shielding of chemical components in garnet cores and in other minerals) and, most importantly, uncertainty of the thermodynamic data. This particularly concerns the influence of minor elements such as Ti, F, Fe3+ on melt, amphibole and titanite compositions, as well as "extending" the application of melt thermodynamic parameters beyond the specified compositional range. For instance, the calculated amphibole compositions deviate from the measured ones, and because of the high modal content of amphibole, this effect may be more important than the garnet shielded from the real bulk reactive composition. Finally, the water content and its variation during changing P-T can only be estimated. Accordingly, forward modelling of the Sabzevar granulites can be considered as tentative only. Nonetheless, general validity of the obtained pseudosection to constraint the P-T path of the Sabzevar granulites can be derived from garnet with zoning pat-

tern such as Ng353_grt1 (cfr. Fig. 9b of the submitted typescript). This garnet type is facing into a leucosome rim and shows no or only minor resorption. Its outer rim is characterized by a significant increase in Ca (up to 0.9 c.f.u.), compensated be a decrease in Mg. Obviously, in this case the garnet outer rim equilibrated with melt during cooling. Considering the calculated content of garnet, this zoning type indicates pressure increase during cooling, compatible with an anti-clockwise P-T path (cfr. Fig. 11a of the submitted typescript). In the rock matrix, rutile is almost completely replaced by ilmenite. Rutile only survives as shielded (mainly mono-phase) inclusion in garnet or in large ilmenite aggregates. The cooling path is also constrained by the preservation of plagioclase in the matrix assemblages (Fig. 11a). Therefore, in the revised version we would emphasize that (i) our forward modelling calculations should be considered as semi-quantitative, (ii) the calculated isopleths do not meet completely the measured ones, (iii) to qualify the derived P-T path as tentative (but, however, being consistent with the conventional thermobarometry and Thermocalc results), and (iv) sources of uncertainty will be discussed. The general aspect of the P-T path, however, is expected to be quite well constrained, since garnet growth during melt crystallisation demands an episode of some P increase during cooling, according to the %grt isopleths.

Finally, following the Referee's suggestion, we will present a synthetic subduction/dynamothermal sole model for the Sabzevar granulites (see attached fig. 13)

Interactive comment on Solid Earth Discuss., 3, 477, 2011.

Sample	Longitude (E)	Latitude (N)	Texture	Rock type	Am1	Am2	Am3	Am4	Cpx	Grt	Pl	Ilm	Rt	Ttn	Chl	Prh	Zeo
Ng353	57° 21′ 19.7′′	36° 11′ 48.3′′	weak foliation	Leucosome - bearing	o	++	o	+	++	++	++	++	o	o	o	-	o
Ng421	57° 19′ 35.4′′	36° 23′ 8.1′′	Cpx and Amph layering	Leucosome-free	o	++	-	-	++	++	++	++	o	o	o	-	o
Eg354d	57° 22′ 24.5′′	36° 22′ 11.7′′	weak foliation	Leucosome-free	o	++	++	++	++	++	+	+	o	o	+	+	+
Sz290	57° 08′ 52.4′′	36° 28′ 11.4′′	weak foliation	Leucosome-free	-	++	++	++	++	++	o	o	o	-	+	+	+
Ng360	57° 01′ 35.5′′	36° 22′ 33.4′′	weak foliation	Leucosome - bearing	o	++	o	-	++	++	++	+	o	o	o	-	-
Ng362	57° 20′ 33.2′′	36° 22′ 53.9′′	weak foliation	Leucosome - bearing	o	++	o	+	++	++	++	+	o	o	o	-	-
368c	57° 09′ 52.4′′	36° 27′ 39.1′′	decussate fabric	Leucosome-free	o	++	+	+	++	++	o	+	-	o	o	-	o
Sz283	57° 08′ 52.4′′	36° 28′ 8.4′′	penetrative foliation	Leucosome-free	-	++	-	-	-	-	++	o	-	-	o	o	o
272	57° 09′14.3′′	36° 28′ 28.1′′	weak foliation	Leucosome - bearing	o	++	-	+	++	++	++	+	o	o	o	o	-
Ng351	57° 21′ 40.4′′	36° 21′ 45.7′′	decussate fabric	Leucosome-free	-	++	+	+	++	++	o	o	o	o	o	o	o
Sz 403	57°08′ 05.2′′	36°28′ 1.3′′	decussate fabric	Leucosome-free	o	++	-	o	-	+	o	+	-	-	-	-	-

++ major constituent; + minor constituent; o accessory phase; – not observed;

Fig. 1. new Table 1

Table 4- Relations between metamorphic stages and mineral growth in the Sabzevar granulites

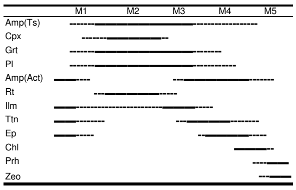

Fig. 2. new Table 4

Table 5 - Synoptic results of the conventional and multi-equilibrium thermobarometry applied to the Sabzevar granulites

		Conventional thermobarometry									THERMOCALCv3.26$^{(*)}$
		Temperature (°C)						Pressure (GPa)			PT best fit (GPa; °C)
		Grt-Cpx		Grt-Amp	Zr-in-Rt			Grt-Cpx-Pl-Qz		Grt-Amp-Pl	
Metamorphic stage	Sample	KR_a	EG	KR_b	W06	F&W07	T07	PN	E	KS	
M2a											
	NG353			640-750 (N=7) (Grt$_{core}$-Amp$_1$)						6.4-4.7 $^{(§§§)}$(N=2) (Grt$_{core}$-Amp$_1$-Pl$_1$)	0.8±0.1; 644±117 (Grt$_{core}$-Amp$_1$-Pl$_1$-Ilm$_1$-Ttn$_1$-Qz)
M2b											
	SZ290	706 $^{(§)}$ (N= 15) (Grt$_{rim}$-Cpx$_2$)	733 $^{(§)}$ (N =15)					1.3 $^{(§§)}$ (N=9) (Grt$_{rim}$-Cpx$_2$-Pl$_2$-Qz)	1.3$^{(§§)}$(N=9)		1.2±0.2; 740±105 (Grt$_{rim}$-Cpx$_2$-Pl$_2$-Rt-Qz)
	NG353	737$^{(§)}$ (N=13) (Grt$_{rim}$-Cpx$_2$)	769 $^{(§)}$ (N=13)		702-803 (N=24)	701-802 (N=24) (Rt in Grt$_{rim}$ or in matrix)	714-809$^{(§)}$ (N=24)	1.1$^{(§§)}$(N=17) (Grt$_{rim}$-Cpx$_2$-Pl$_2$-Qz)	1.2 $^{(§§)}$(N=17)		1.0±0.1; 742±74 (Grt$_{rim}$-Cpx$_2$-Pl$_2$-Rt-Qz)
	EG354	715$^{(§)}$(N=11) (Grt$_{rim}$-Cpx$_2$)	743 $^{(§)}$(N=11)					1.1 $^{(§§)}$(N=11) (Grt$_{rim}$-Cpx$_2$-Pl$_2$-Qz)	1.2 $^{(§§)}$(N=11)		
	NG421	724 $^{(§)}$(N=3) (Grt$_{rim}$-Cpx$_2$)	789 $^{(§)}$(N=3)								1.3±0.4; 861±73 (Grt$_{rim}$-Cpx$_2$-Pl$_2$-Ep-Amp$_2$-Qz)
M3											
	SZ290									0.54-0.35$^{(§§§)}$(N=3) (Grt$_{rim}$-Amp$_3$-Pl$_3$)	
	NG353			574-631 (N=7) (Grt$_{rim}$-Amp$_3$)						0.58-0.39$^{(§§§)}$(N=8) (Grt$_{rim}$-Amp$_3$-Pl$_3$)	
	EG354			611-677 (N=10) (Grt$_{rim}$-Amp$_3$)						0.62-0.44$^{(§§§)}$(N=6) (Grt$_{rim}$-Amp$_3$-Pl$_3$)	

(*) Representative results; $^{(§)}$: at 0.1 GPa; $^{(§§)}$: at 750 °C; $^{(§§§)}$: from 500 to 700 °C.
KR_a: Krogh Ravna (2000a); KR_b: Krogh Ravna (2000b); EG: Ellis and Green (1979); W06: Watson et al. (2006); F&W07: Ferry and Watson (2007); T07: Tomkins et al. (2007); PN: Perkins and Newton (1981); E: Eckert et al. (1981); KS: Kohn and Spear (1990); (N=7): number of estimates

Fig. 3. new Table 4

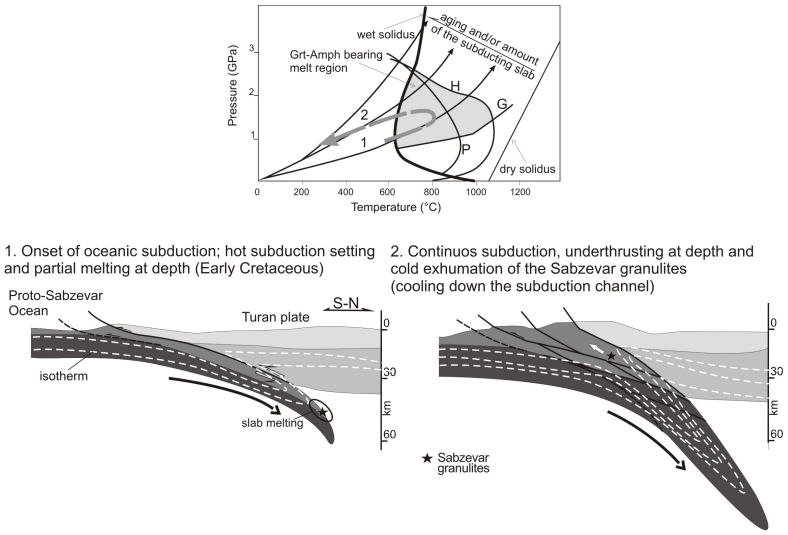

Fig. 13 - Conceptual two-stage geodynamic model to accomplish for the anticlockwise P-T evolution recorded by the Sabzevar granulites. This P-T path is interpreted as consequence of transition from an infant to a mature stage of subduction of the Proto-Sabzevar Ocean below the Turan plate. The top panel (modified and re-adapted after Peackock et al., 1994 and Martin, 1999) show the dry and wet solidus of tholeiite and the inferred P-T trajectories and geothermal gradients in the subduction channel as a function of the age and/or amount of the subducted oceanic lithosphere. Trajectories 1 and 2, refers to a nascent and mature subduction, respectively. Slab melting is predicted only when young lithosphere subducts or at the eraly stages of subduction. The dashed grey arrow schematically depicts the P-T evolution of the Sabzevar granulites . Key to labels: G, and P, line delimiting garnet and plagioclase stability, respectively; H, horneblende-out.

Fig. 4. New Figure 13 (geodynamic model)